# Mechanistic Detail Revealed via Comprehensive Kinetic Modeling of [*rac*-C$_2$H$_4$(1-indenyl)$_2$ZrMe$_2$]-Catalyzed 1-Hexene Polymerization

Krista A. Novstrup,[†] Nicholas E. Travia,[‡] Grigori A. Medvedev,[†] Corneliu Stanciu,[‡] Jeffrey M. Switzer,[†] Kendall T. Thomson,[†] W. Nicholas Delgass,[†] Mahdi M. Abu-Omar,*[,‡] and James M. Caruthers*[,†]

*School of Chemical Engineering and Department of Chemistry, Purdue University, West Lafayette, Indiana 47907*

Received July 28, 2009; E-mail: caruther@purdue.edu; mabuomar@purdue.edu

***Abstract:*** Thorough kinetic characterization of single-site olefin polymerization catalysis requires comprehensive, quantitative kinetic modeling of a rich multiresponse data set that includes monomer consumption, molecular weight distributions (MWDs), end group analysis, etc. at various conditions. Herein we report the results obtained via a comprehensive, quantitative kinetic modeling of all chemical species in the batch polymerization of 1-hexene by *rac*-C$_2$H$_4$(1-Ind)$_2$ZrMe$_2$ activated with B(C$_6$F$_5$)$_3$. While extensive studies have been published on this catalyst system, the previously acknowledged kinetic mechanism is unable to predict the MWD. We now show it is possible to predict the entire multiresponse data set (including the MWDs) using a kinetic model featuring a catalytic event that renders 43% of the catalyst inactive for the duration of the polymerization. This finding has significant implications regarding the behavior of the catalyst and the polymer produced and is potentially relevant to other single-site polymerization catalysts, where it would have been undetected as a result of incomplete kinetic modeling. In addition, comprehensive kinetic modeling of multiresponse data yields robust values of rate constants (uncertainties of less than 16% for this catalyst) for future use in developing predictive structure−activity relationships.

## Introduction

Single-site catalysis of olefin polymerization is an active research area because of the precisely engineered physical properties of the polymers produced and the possibility of designing systems from first principles.[1−13] Because there is a single catalytic site, kinetic studies can give fundamental insight as to why a catalyst system produces a particular molecular architecture in the polymer. It is through this detailed mechanistic/kinetic understanding of catalyst systems that catalyst performance can be optimized[14] and in principle quantitative structure−activity relationships developed for rational design of new single-site catalysts.[15,16]

Mechanistic detail in the kinetic model is obviously essential for being able to use the information to rationally design new catalysts. When a less than complete catalyst description is used, the applicability of the model to scaling-up/optimization of a polymerization process or using the information to predict new catalyst structures becomes difficult or even impossible. This was illustrated by Stoveng and co-workers,[16] who showed that a quantitative structure−activity relationship based on catalyst activity (i.e., single-point measurement of the polymer yield per amount of catalyst per polymerization time) was qualitatively less accurate than one based on the true propagation rate. This was a result of the fact that characterization of polymerization kinetics via activity can result in considerable ambiguity, because the polymer yield used to calculate activity is dependent on multiple processes including the rate of initiation, termination, and deactivation in addition to the rate of propagation.

[†] School of Chemical Engineering.
[‡] Department of Chemistry.
(1) Alt, H. G.; Koppl, A. *Chem. Rev. (Washington, DC, U.S.)* **2000**, *100*, 1205–1221.
(2) Angermund, K.; Fink, G.; Jensen, V. R.; Kleinschmidt, R. *Chem. Rev. (Washington, DC, U.S.)* **2000**, *100*, 1457–1470.
(3) Bochmann, M. *J. Chem. Soc., Dalton Trans.* **1996**, 255–270.
(4) Bochmann, M. *J. Organomet. Chem.* **2004**, *689*, 3982–3998.
(5) Brintzinger, H. H.; Fischer, D.; Mulhaupt, R.; Rieger, B.; Waymouth, R. M. *Angew. Chem., Int. Ed.* **1995**, *34*, 1143–1170.
(6) Chen, E. Y. X.; Marks, T. J. *Chem. Rev. (Washington, DC, U.S.)* **2000**, *100*, 1391–1434.
(7) Coates, G. W. *Chem. Rev. (Washington, DC, U.S.)* **2000**, *100*, 1223–1252.
(8) McKnight, A. L.; Waymouth, R. M. *Chem. Rev. (Washington, DC, U.S.)* **1998**, *98*, 2587–2598.
(9) Mohring, P. C.; Coville, N. J. *Coord. Chem. Rev.* **2006**, *250*, 18–35.
(10) Prashar, S.; Antinolo, A.; Otero, A. *Coord. Chem. Rev.* **2006**, *250*, 133–154.
(11) Rappe, A. K.; Skiff, W. M.; Casewit, C. J. *Chem. Rev. (Washington, DC, U.S.)* **2000**, *100*, 1435–1456.
(12) Resconi, L.; Cavallo, L.; Fait, A.; Piemontesi, F. *Chem. Rev. (Washington, DC, U.S.)* **2000**, *100*, 1253–1345.
(13) Wang, B. *Coord. Chem. Rev.* **2006**, *250*, 242–258.

(14) Matos, V.; Neto, A. G. M.; Nele, M.; Pinto, J. C. *J. Appl. Polym. Sci.* **2002**, *86*, 3226–3245.
(15) Manz, T. A.; Phomphrai, K.; Medvedev, G. A.; Krishnamurthy, B. B.; Sharma, S.; Haq, J.; Novstrup, K. A.; Thomson, K. T.; Delgass, W. N.; Caruthers, J. M.; Abu-Omar, M. M. *J. Am. Chem. Soc.* **2007**, *129*, 3776–3777.
(16) Stovneng, J. A.; Stokvold, A.; Thorshaug, K.; Rytter, E. In *Metalorganic Catalysts for Synthesis and Polymerization: Recent Results by Ziegler-Natta and Metallocene Investigations*; Kaminsky, W., Ed.; Springer-Verlag: Berlin, Germany, 1999; pp 274−282.

A complete mechanistic/kinetic description requires probing the polymerization and resultant polymer via a number of different techniques, the collection of which we now refer to as multiresponse data. A number of approaches for collecting and analyzing multiresponse data have been published. Primarily these studies report monomer consumption or polymer yield versus time for semibatch or batch polymerization experiments, where the initiation,[17−21] propagation,[15,17,18,20−24] and deactivation[25,26] rate constants are abstracted from these data. In several cases the analyses also include determination of the ratio of the propagation rate to the chain transfer rate based on the degree of polymerization versus monomer concentration data[17,21,27,28] or measurement of the rate of formation of end groups to infer chain transfer mechanisms and rate constants.[18,20] While the evolution of the molecular weight distribution (MWD) during polymerization provides a wealth of kinetic information,[29] it is typically (i) overlooked completely, (ii) considered only at the end of the reaction, or (iii) reduced to a molecular weight average (i.e., $M_n$ or $M_w$) to eliminate the complexity arising in analyzing the full MWD.[30]

When multiresponse data are collected, the different data response types are generally analyzed separately.[20,21] This approach of individual measurements and simplified analysis has yielded mechanistic insight and reasonable approximations of rate constants, but this piecemeal approach is susceptible to errors caused by ignoring the fact that the individual reactions are coupled, occurring simultaneously during the polymerization, with a collective effect on the molecular components of the multiresponse data. A limited number of single-site and heterogeneously catalyzed polymerization studies have employed a more holistic modeling approach which includes simultaneous consideration of multiple types of data responses to obtain more complete kinetic descriptions of polymerization catalyst systems.[14,31−35] However, these studies did not use the full MWD, thus reducing the informational content of the data

and potentially limiting the ability of the modeling activity to distinguish mechanistic details. Computational tools now exist to kinetically model the full MWD, enabling the simultaneous fitting of multiresponse data.[36] In our opinion, a comprehensive, quantitative kinetic modeling approach for the study of single-site polymerization catalysts will lead to an improved kinetic/mechanistic description of each catalyst, potentially exposing catalytically important events that could be missed using only a simplified kinetic analysis.

To illustrate the necessity for employing a comprehensive kinetic analysis for single-site olefin polymerization, in this paper we will focus on arguably the most extensive kinetic study performed to date for a single monomer/catalyst/activator system—1-hexene polymerization by (EBI)ZrMe₂ (EBI = *rac*-C₂H₄(1-Ind)₂) activated with B(C₆F₅)₃ as reported by Landis and co-workers.[19,20,37−41] These studies included independent measurement of the rate constants for activation and initiation.[20] The propagation rate constant was inferred from both monomer consumption and polymer yield experiments that used the independently measured initiation rate constant.[20] The rate constants for vinylene and vinylidene double bond formation were also independently measured.[20] In addition to the measured rate constants, specifically designed experiments were used to probe details of the propagation mechanism (i.e., intermittent versus continuous)[41] and the reactivity of 2,1-misinserted species.[39]

Landis et al.[20] combined the mechanistic details and measured rate constants obtained from the individual experiments to propose a specific kinetic model (see Scheme 1 and Table 1) to describe 1-hexene polymerization by the (EBI)ZrMe₂/B(C₆F₅)₃ catalyst system. In this kinetic model, catalyst activation is not explicitly modeled as it is considered fast and complete. Vinylidene double bonds are formed by β-hydride elimination, and two variations of vinylene double bond formation are proposed. The general vinylene reaction reflects the second-order rate constant reported by Landis for vinylene formation. The specific mechanism of vinylene formation can be interpreted as either a single bimolecular reaction or a multireaction mechanism containing 2,1-misinsertion followed by β-hydride elimination (see "Vinylene Reaction Specific" in Scheme 1). This detailed kinetic model was then used to predict the experimental MWDs for polymerizations from three different initial monomer concentrations.[20] Landis et al. recognized that the experimental MWDs have a higher number-average molecular weight and are broader than those predicted. This discrepancy was attributed to "systematic errors in the GPC calibration of absolute molecular weights". However, an alternative explanation is that this discrepancy is not just an artifact of the GPC analysis but rather indicative of an additional mechanism not currently accounted for in the kinetic model.

In this paper we will establish that in addition to the reactions described in Scheme 1 a new rapid catalytic step resulting in inactivation of approximately half the catalyst is required to

(17) Busico, V.; Cipullo, R.; Esposito, V. *Macromol. Rapid Commun.* **1999**, *20*, 116–121.

(18) Klamo, S. B. Ph.D. Dissertation, California Institute of Technology, 2005.

(19) Liu, Z.; Somsook, E.; Landis, C. R. *J. Am. Chem. Soc.* **2001**, *123*, 2915–2916.

(20) Liu, Z.; Somsook, E.; White, C. B.; Rosaaen, K. A.; Landis, C. R. *J. Am. Chem. Soc.* **2001**, *123*, 11193–11207.

(21) Song, F.; Hannant, M. D.; Cannon, R. D.; Bochmann, M. *Macromol. Symp.* **2004**, *213*, 173–185.

(22) Keaton, R. J.; Jayaratne, K. C.; Henningsen, D. A.; Koterwas, L. A.; Sita, L. R. *J. Am. Chem. Soc.* **2001**, *123*, 6197–6198.

(23) Mehrkhodavandi, P.; Schrock, R. R.; Pryor, L. L. *Organometallics* **2003**, *22*, 4569–4583.

(24) Sillars, D. R.; Landis, C. R. *J. Am. Chem. Soc.* **2003**, *125*, 9894–9895.

(25) Dornik, H. P.; Luft, G.; Rau, A.; Wieczorek, T. *Macromol. Mater. Eng.* **2004**, *289*, 475–479.

(26) Wester, T. S.; Johnsen, H.; Kittilsen, P.; Rytter, E. *Macromol. Chem. Phys.* **1998**, *199*, 1989–2004.

(27) Chen, M. C.; Roberts, J. A. S.; Marks, T. J. *J. Am. Chem. Soc.* **2004**, *126*, 4605–4625.

(28) Naga, N.; Mizunuma, K. *Polymer* **1998**, *39*, 5059–5067.

(29) Haq, J. Master Thesis, Purdue University, 2006.

(30) Wulkow, M. *Macromol. Theory Simul.* **1996**, *5*, 393–416.

(31) Quevedo-Sanchez, B.; Nimmons, J. F.; Coughlin, E. B.; Henson, M. A. *Macromolecules* **2006**, *39*, 4306–4316.

(32) Matos, V.; Neto, A. G. M.; Pinto, J. C. *J. Appl. Polym. Sci.* **2001**, *79*, 2076–2108.

(33) Luo, Z.-H.; Wang, W.; Su, P.-L. *J. Appl. Polym. Sci.* **2008**, *110*, 3360–3367.

(34) Kou, B.; McAuley, K. B.; Hsu, J. C. C.; Bacon, D. W. *Macromol. Mater. Eng.* **2005**, *290*, 537–557.

(35) Belelli, P. G.; Ferreira, M. L.; Lacunza, M. H.; Damiani, D. E.; Brandolin, A. *Polym. Eng. Sci.* **2001**, *41*, 2082–2094.

(36) Cao, J.; Goyal, A.; Novstrup, K. A.; Midkiff, S. P.; Caruthers, J. M. *Int. J. Parallel Program.* **2009**, *37*, 127–152.

(37) Landis, C. R.; Liu, Z.; White, C. B. *Polym. Prepr. (Am. Chem. Soc., Div. Polym. Chem.)* **2002**, *43*, 301–302.

(38) Landis, C. R.; Rosaaen, K. A.; Uddin, J. *J. Am. Chem. Soc.* **2002**, *124*, 12062–12063.

(39) Landis, C. R.; Sillars, D. R.; Batterton, J. M. *J. Am. Chem. Soc.* **2004**, *126*, 8890–8891.

(40) Landis, C. R.; Christianson, M. D. *Proc. Natl. Acad. Sci. U.S.A.* **2006**, *103*, 15349–15354.

(41) Landis, C. R.; Rosaaen, K. A.; Sillars, D. R. *J. Am. Chem. Soc.* **2003**, *125*, 1710–1711.

**Scheme 1**
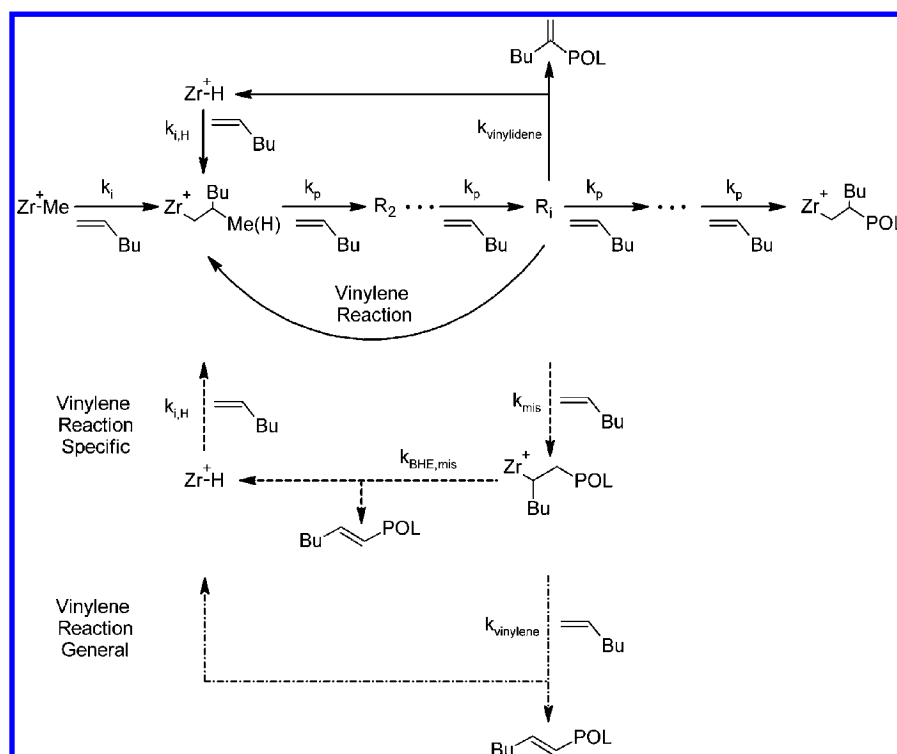


**Table 1.** Rate Constant Values for the Kinetic Model Given in Scheme 1

| parameter set | units | Landis et al.[a] | PASM[b] |
|---|---|---|---|
| $k_i$ | $M^{-1} s^{-1}$ | 0.033 | 0.031 |
| $k_p$ | $M^{-1} s^{-1}$ | 2.2 | 3.7 |
| $k_{vinylidene}$ | $s^{-1}$ | 0.00066 | 0.0024 |
| $k_{vinylene}$ | $M^{-1} s^{-1}$ | 0.0016 | 0.014 |
| $X_{active}$ | dimensionless | 1.0 | 0.57 |
| total SSE[c] | dimensionless | 43 | 1.9 |

[a] From ref 20. [b] This work. PASM = partial active site model. [c] SSE = sum of squared error.

describe 1-hexene polymerization by (EBI)ZrMe$_2$ activated with B(C$_6$F$_5$)$_3$. This discovery was made via comprehensive modeling of the rich multiresponse data set, as compared to previous studies based on individual data analysis that did not quantitatively predict the MWD; specifically, the MWD (even in the presence of potential systematic GPC analysis errors) provides quantitative information that points toward a hitherto unidentified mechanistic step. These results will clearly show that comprehensive, quantitative kinetic analysis is every bit as important a tool in determination of polymerization mechanisms as direct spectroscopic measurements of reactants, products, and intermediates. Finally, the simultaneous modeling of rich multiresponse data was found to give robust rate constant values that can then be used in future investigation of how changes in the molecular structure of the catalyst affect the kinetics of the polymerization.

## Experimental Methods

**General Conditions.** All experiments employing metal complexes were performed under a dry nitrogen atmosphere in a glovebox or at a vacuum manifold using techniques for handling air-sensitive compounds. Toluene and diethyl ether were distilled over Na/benzophenone and stored over molecular sieves. *rac*-Ethylene(bisindenyl)zirconium dichloride was purchased from

Strem and used as received. 1-Hexene was purchased from Aldrich, purified by distillation over a small amount of dimethylbis(cyclopentadienyl)zirconium, and stored over molecular sieves. Tris(pentafluorophenyl)boron was purchased from Strem and purified by sublimation. Diphenylmethane was purchased from Aldrich and stored over molecular sieves. $d_1$- and $d_4$-methanol were purchased from Cambridge Isotopes and either used immediately upon opening or wrapped in Parafilm for storage absent of light. Methyllithium (1.6 M in diethyl ether) was purchased from Aldrich and used as received. $^1$H and $^2$H NMR experiments were performed on a Varian INOVA300 MHz or Bruker DRX500 MHz spectrometer.

**Synthesis of *rac*-(C$_2$H$_4$(1-indenyl)$_2$)ZrMe$_2$.** The procedure is based on that in the literature.[42] In a typical synthesis, a 100 mL flask was charged with *rac*-(C$_2$H$_4$(1-indenyl)$_2$)ZrCl$_2$ (1.013 g, 2.42 mmol), 30 mL of diethyl ether, and a stir bar and fitted with a rubber septum. The resulting solution was stirred and cooled to −78 °C while methyllithium (5.57 mmol) was introduced dropwise. The reaction was allowed to warm to room temperature, stirred for 4 h or sometimes overnight, and then filtered through Celite into a separate flask, yielding a dark yellow solution. The solution was concentrated in vacuo to about 10 mL and placed into a −2 °C freezer. Yellow-orange crystals formed within 3 days, and a second crop was sometimes obtained in combined 20% yield. NMR results are consistent with what has been reported.

**Polymerization of 1-Hexene.** The procedure for manual quench is based on that in the literature.[20] For a typical polymerization, (EBI)ZrMe$_2$ (0.0282 g, 0.0747 mmol) was dissolved in 2.0 mL of toluene in a small vial that was sealed with a screw-cap septum. To a 100 mL flask was added a 28.0 mL toluene, tris(pentafluorophenyl)boron (0.0382 g, 0.0747 mmol), diphenylmethane (0.6 mL, 3.6 mmol), and 1-hexene (3.75 mL, 30.0 mmol) solution. Both solutions were cooled to 0 °C, and a small sample of 1-hexene solution was removed for initial NMR analysis. The catalyst precursor solution was added to the activator/monomer solution. The resulting dark orange solution was allowed to stir while ca. 1 mL aliquots were removed at selected times and each was injected into an NMR tube containing 0.1 mL of $d_4$-methanol and 0.3 mL

(42) Bochmann, M.; Lancaster, S. J. *Organometallics* **1993**, *12*, 633–640.

of $d_8$-toluene (for locking the spectrometer). The measured exotherm for the reaction was never more than 2 °C. The consumption of 1-hexene was quantified by $^1$H NMR against the diphenylmethane internal standard, and each sample was prepared for GPC analysis by evaporation over mild heat before dissolution in hexane and filtration through an alumina plug to remove the catalyst. Evaporation of solvent yielded clear, colorless polyhexene with >95% retention.

In the case of $^2$H analysis, the entire reaction was quenched at a selected time with $d_1$-methanol and the entire polymer was worked up, dissolved in $CH_2Cl_2$, and diluted to mark in a 5.00, 10.00, or 25.00 mL volumetric flask. Dissolution was difficult at higher monomer conversions. Therefore, more dilute samples were needed to prevent viscosity problems. $d_6$-Benzene was used as an internal standard, and the method of standard additions was used to quantify $^2$H NMR.

In the case of $^1$H NMR analysis of vinyl functional groups, either a small quenched aliquot or the entire batch was worked up as described above. Diphenylmethane was used as an internal standard, and the method of standard additions was employed.

**Gel Permeation Chromatography.** Gel permeation chromatography was performed on a triple-detector Waters GPCV 2000 equipped with a differential RI detector, a triple capillary flow-through viscometer, and a Precision Detectors PD2040 two-angle light scattering detector. Two Polymer Laboratories PLGel 5 $\mu$M Mixed-C columns were used, and a universal calibration curve was constructed from 10 narrow polystyrene standards (580−3114000 g/mol) also obtained from Polymer Laboratories. The "systematic approach" to calibration described by Mourey and Balke[43] was used to minimize systematic uncertainties in the MWD analysis. The broad polystyrene sample NBS 706a was used to validate the inter-detector time. Samples were run in distilled THF at 45 °C and 1 mL/min. Polystyrene standards were run at a concentration of 0.02−0.9% (w/v), and polyhexene sample concentrations were approximately 0.2% (0.1% = 1 mg/mL). Exact polyhexene sample concentrations were determined from the differential RI detector using a specific refractive index of 0.076 mL/g for polyhexene in THF. For a more complete description of the GPC analysis see the Supporting Information.

**Kinetic Modeling.** For each kinetic model considered, the associated population balance equations, which are a set of ordinary differential equations (ODEs), must be generated. The solution of the ODEs is then optimized with respect to a given set of experimental data to determine the optimal set of model parameters (i.e., rate constants, etc.) for that specific kinetic model. The population balance includes a differential equation for each species in the polymerization for every possible chain length. A kinetic model containing activation, initiation, and propagation has the following elementary reactions:

$$C + A \xrightarrow{k_a} C^* \tag{1}$$

$$C^* + M \xrightarrow{k_i} R_1 \tag{2}$$

$$R_n + M \xrightarrow{k_p} R_{n+1} \tag{3}$$

The population balance equations are written as the following using mass action kinetics:

$$d[A]/dt = -k_a[A][C] \tag{4}$$

(43) Mourey, T. H.; Balke, S. T. In *Chromatography of Polymers: Characterization by SEC and FFF*; Provder, T., Ed.; ACS Symposium Series 521; American Chemical Society: Washington, DC, 1993; pp 180−198.

$$d[C]/dt = -k_a[A][C] \tag{5}$$

$$d[C^*]/dt = k_a[A][C] - k_i[C^*][M] \tag{6}$$

$$d[M]/dt = -k_i[C^*][M] - k_p[M](\sum_{n=1}^{L_{max}} [R_n]) \tag{7}$$

$$d[R_1]/dt = k_i[C^*][M] - k_p[R_1][M] \tag{8}$$

$$d[R_n]/dt = k_p([R_{n-1}] - [R_n])[M] \qquad 2 \le n \le L_{max} \tag{9}$$

where $k_a$, $k_i$, and $k_p$ are the activation, initiation, and propagation rate constants, respectively, and the species are a precatalyst (C), an activator (A), an activated catalyst (C*), a monomer (M), and a living polymer that is *n*-mers long ($R_n$). Numerical calculation requires specification of a maximum chain length of $L_{max}$, which is set to a value much larger than that of any experimentally observed species and sufficiently large to ensure conservation of mass during simulation (i.e., no appreciable amount of polymer chains of length greater than $L_{max}$ are predicted). For the polymers analyzed in this paper $L_{max}$ was on the order of 2500. Also, for the catalyst system under consideration in this paper, activation is considered complete and fast on the basis of previous literature results;[20] therefore, $[C^*]_0 = [C]_0$, eliminating the requirement to explicitly include the catalyst activation reaction in the kinetic models. In addition to the activation, initiation, and propagation steps described above, we have added three additional reactions as indicated in Scheme 1 to create the partial active site kinetic model. A $\beta$-hydride elimination reaction (eq 10) followed by reinitiation of the zirconium hydride (eq 11) was added along with a general bimolecular vinylene formation reaction (eq 12):

$$R_n \xrightarrow{k_{vinylidene}} C^*_H + SR_n \tag{10}$$

$$C^*_H + M \xrightarrow{k_{i,H}} R_1 \tag{11}$$

$$R_n + M \xrightarrow{k_{vinylene}} R_1 + SP_n \tag{12}$$
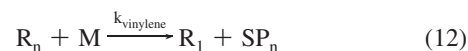
where $k_{vinylidene}$, $k_{i,H}$, and $k_{vinylene}$ are the $\beta$-hydride elimination, zirconium hydride reinitiation, and bimolecular vinylene formation rate constants, respectively, and the additional species are vinylidene-terminated chains ($SR_n$), vinylene-terminated chains ($SP_n$), and zirconium hydride species ($C^*_H$). In addition, the assumption that $[C^*]_0 = [C]_0$ is modified to $[C^*]_0 = X_{active}[C]_0$, where $X_{active}$ represents the fraction of catalyst that actively undergoes polymerization during the reaction. Inclusion of these reactions and species in the kinetic model requires the creation of additional ODEs for $SR_n$, $SP_n$, and $C^*_H$ (see the Supporting Information for ODEs) as well as modification of the ODEs in eqs 4−9 above.

To rapidly generate, without error, the kinetic expressions and associated ODEs for various postulated mechanisms, we have developed a suite of computer-aided reaction modeling design tools that we refer to as the RMSuite.[36] The RMSuite included a chemical compiler that allows the researcher to write the various reaction mechanisms in a near-English-language format and then automatically generate both the kinetic expressions and associated ODEs for the approximately 10 000 species in the model. The parameters in the ODEs can then be regressed from the multiresponse data via a parallelized optimization routine. In this work we employed the Runge−Kutta−Fehlberg (4, 5) solver from the GNU scientific library to calculate numerical solutions to the ODEs. Optimization of the rate constants was performed with a parallelized Levenberg−Marquardt optimization algorithm.[44] The objective function is a sum of squared errors in which each data response (i.e., monomer consumption curve, MWD, etc.) is assigned its own weighting factor, which includes normalization by the number of data points
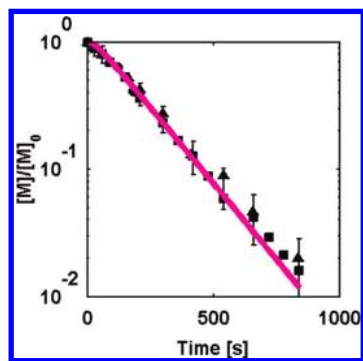
**Figure 1.** Monomer consumption from two replicate experiments (■, ▲) compared to the Landis et al. model[20] prediction (pink line). Error bars represent a 98% confidence interval. Conditions: 0 °C, toluene, [(EBI)-ZrMe$_2$]$_0$ = [B(C$_6$F$_5$)$_3$]$_0$ = 2.49 mM, [1-hexene]$_0$ = 1.0 M.

in the particular response and scaling of the error by the experimental standard deviation for that data response. Further weighting could be assigned to each data response by the researcher to give greater importance to certain data types (e.g., monomer consumption over the MWD). Details of the weighting can be found in the Supporting Information. Finally, a number of initial parameter guesses in the Levenberg–Marquardt algorithm were used to increase confidence that the true global minimum was determined.

## Results

**Verification of the Inadequacy of the Literature Model.** Batch polymerization of 1-hexene (1.0 M) by (EBI)ZrMe$_2$ (2.49 mM) and B(C$_6$F$_5$)$_3$ (2.49 mM) in toluene at 0 °C was performed to verify the previously observed[20] discrepancy between the experimental and predicted MWDs for this catalyst system. The polymerization was run to more than 90% conversion of monomer (Figure 1), giving a rate of monomer consumption consistent with that predicted using the previously reported rate constants of Landis et al.[20] The MWD was sampled at 100 s (i.e., 30% monomer conversion), 220 s (60%) and 800 s (90%). Figure 2 plots the previously reported experimental MWDs[20] alongside those measured by our group. Consistent with the previous observation, our experimental data show a broader, higher MWD than predicted from the model proposed by Landis et al.[20] In addition, our data show that the discrepancy persists throughout the duration of the polymerization.

To eliminate concerns that the MWD discrepancy is merely a consequence of inaccuracies occurring during GPC analysis, the experiment was performed multiple times to assess experimental reproducibility between catalyst batches, the reaction scale, etc., and a thorough study was performed on the sources, magnitude, and impact of systematic errors in the GPC analysis. The experimental reproducibility is illustrated by the 100 s data in Figure 2, where MWDs from three replicate polymerization experiments and two repeat GPC measurements are plotted. The overlay of the MWDs shows a high level of reproducibility in the MWD measurement. The molecular weight averages for these measurements are reported in Table 2 and reinforce the visual picture, showing the model prediction clearly lies outside any experimental uncertainties. Likewise, systematic errors in the GPC analysis were found to yield errors of a magnitude similar to that seen for the reproducibility experiments (see the

(44) Cao, J.; Novstrup, K. A.; Goyal, A.; Midkiff, S. P.; Caruthers, J. M. In *ICS'09*, Proceedings of the 23rd International Conference on Supercomputing, Yorktown Heights, NY, June 8–12, 2009; Gschwind, M., Nicolau, A., Salapura, V., Moreira, J., Eds.; ACM: New York, 2009; pp 450–459.

Supporting Information for a complete discussion). Thus, it can be stated with confidence that the discrepancy between the experimental and predicted MWDs is clearly outside the reproducibility and systematic analysis errors possible in the GPC measurement. Therefore, the inability of the Landis et al.[20] kinetic model and rate constants to predict the MWD must result from an inadequacy in that particular kinetic model and/or errors in the determination of the rate constants.

**Partial Active Site Kinetic Model.** Comprehensive, quantitative kinetic modeling via simultaneous fitting of the multiresponse polymerization data was used to resolve the MWD discrepancy between the literature model and the experimental data. A number of models were considered to describe the data set keeping in mind the principal of Occam's razor; i.e., the simplest model that can describe the data is preferred. While a model can never be proven correct, a kinetic model was found which is capable of robustly predicting the MWDs reported in Figure 2 while maintaining the same quality of fit in the monomer consumption data and successfully predicting other data types. Figure 3 shows the vastly improved fit given by this model. The prediction given in Figure 3 is the result of optimization of the model parameters using the data presented in Figure 3 and additional data presented below in Figures 4 and 5 and Figures S7, S8, and S9 of the Supporting Information.

The new kinetic model closely resembles the Landis et al.[20] model as it is also specified by the reactions given in eqs 1–3 and 10–12; however, two important distinctions are made between the Landis et al.[20] model and the one used to produce the fit given in Figure 3. First, 43% of the catalyst is inactive toward polymerization beginning in the initial stages of the polymerization and remains inactive for the duration of the reaction. This requirement was incorporated into the Scheme 1 model by inputting a decreased amount of activated catalyst which is allowed to initiate and polymerize (i.e., [(EBI)ZrMe$^+$]$_0$ < [(EBI)ZrMe$_2$]$_0$ instead of [(EBI)ZrMe$^+$]$_0$ = [(EBI)ZrMe$_2$]$_0$). This model will henceforth be referred to as the partial active site model (PASM). The second distinction from the original model by Landis et al.[20] is modification of the rate constant values to reflect the lesser amount of actively polymerizing catalyst.

Figure 3 also showcases the PASM's ability to successfully describe two additional data types. First, the unsaturated end groups were measured by $^1$H NMR. Vinylidene and vinylene double bonds were the dominate groups observed, with mono- and trisubstituted alkenes occurring at less than 5 mol %. Second, the instantaneous concentration of active sites was measured by quenching with MeOD and acquiring a $^2$H NMR spectrum of the polymer. The PASM prediction given in Figure 3 was obtained from summing the concentration of species R$_3$ to R$_{max}$ in Scheme 1. The small oligomers (i.e., those resulting from quenching of R$_1$ and R$_2$ species) were excluded as they are likely lost during workup. It is immediately clear that the measured instantaneous active site concentration is consistent with the PASM requirement of approximately 50% of the catalyst remaining inactive during polymerization. In contrast, both of these experimental data responses are poorly predicted by the Landis et al. model[20] (see the Supporting Information).

The success of the PASM to describe the (EBI)ZrMe$_2$ catalyst system was further probed by using the model to describe data obtained from a variety of initial conditions. Polymerizations were run at five additional initial conditions, systematically changing the initial catalyst concentration (1.00 and 1.66 mM), initial monomer concentration (0.5 M and 12.5 mM), and initial
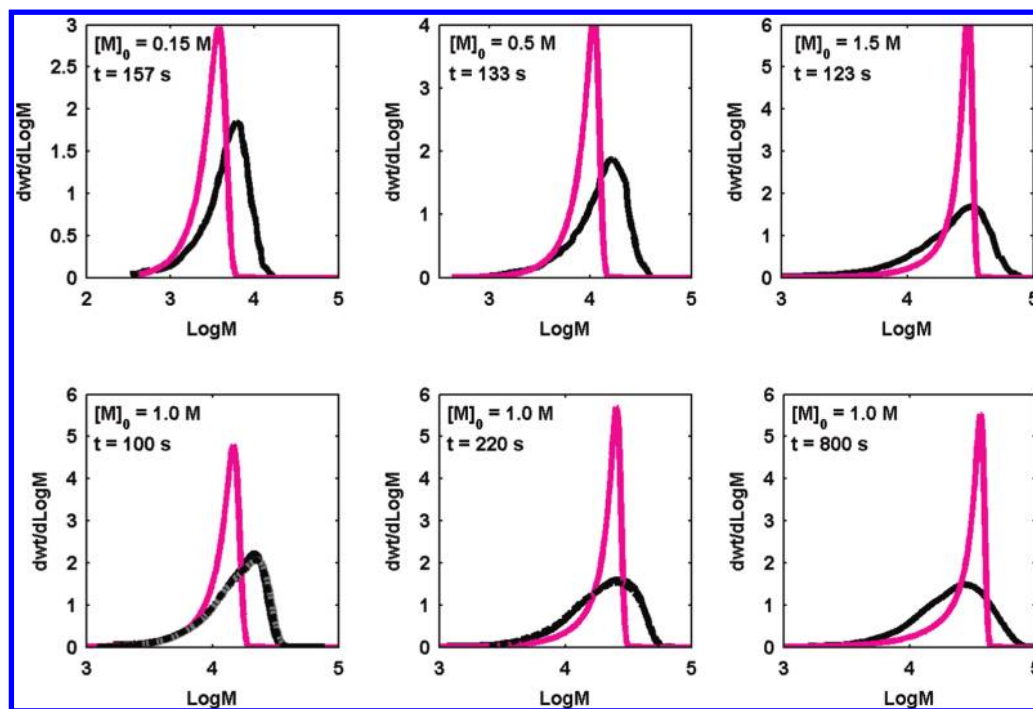
**Figure 2.** (Top) Digitized MWD data obtained from Landis et al.[20] (black line) (6−10% monomer conversion) (0 °C, toluene, [(EBI)ZrMe$_2$]$_0$ = [B(C$_6$F$_5$)$_3$]$_0$ = 0.6 mM). (Bottom) Our measured MWDs sampled at 100 s (30% monomer conversion), 220 s (60%), and 800 s (90%) (0 °C, toluene, [(EBI)ZrMe$_2$]$_0$ = [B(C$_6$F$_5$)$_3$]$_0$ = 2.49 mM). The 100 s plot includes three replicate experiments and two repeat GPC measurements. The 200 s plot includes two replicate experiments. The prediction given by the Landis et al. model[20] (pink line) is plotted for each distribution.

**Table 2.** Experimental Molecular Weight Averages (kg/mol) of the 100 s Polyhexene Sample[a] and Landis et al.[20] Model Prediction

| polymerization | $M_n$ | $M_w$ | PDI |
|---|---|---|---|
| 1 | 12.5 | 16.8 | 1.3 |
| 2 | 11.8 | 16.1 | 1.4 |
| 3 | 12.0 | 15.8 | 1.3 |
| 3 (GPC repeat 1) | 12.3 | 16.5 | 1.3 |
| 3 (GPC repeat 2) | 12.9 | 17.0 | 1.3 |
| Landis et al.[20] model prediction | 10.0 | 12.1 | 1.2 |

[a] Conditions: 0 °C, toluene, [(EBI)ZrMe$_2$]$_0$ = [B(C$_6$F$_5$)$_3$]$_0$ = 2.49 mM, [1-hexene]$_0$ = 1.0 M.

activator concentration (5 mM). Data from two of the polymerizations are given, representative of decreasing the initial catalyst concentration (1.00 mM in Figure 4) and decreasing the initial monomer concentration (0.5 M in Figure 5). The data for the three other polymerizations as well as the prediction given by the PASM are provided in the Supporting Information.

The PASM can describe all these additional experiments, although the deviation of the monomer consumption from the prediction seen in Figure 4 after 1500 s (i.e., 90% monomer conversion) deserves comment. This divergence is attributed to deactivation of the catalyst caused by the introduction of small amounts of moisture during sampling. Lower catalyst concentrations and longer sampling times are more susceptible to the deleterious effect of moisture contamination during sampling as this is also observed after 74% conversion in the 1.66 mM catalyst experiment. However, the initial 90% conversion in the 1.00 mM experiment and the initial 74% conversion in the 1.66 mM experiment show good agreement with the monomer consumption prediction, and the predicted MWDs are in excellent agreement with the experimental data. Finally, the requirement that approximately 50% of the catalyst must be inactive to polymerize persists as the initial monomer, catalyst,

and activator concentrations were each individually altered by a factor of 2 or more.

**Rate Constants and Fraction of Active Sites.** The PASM in Scheme 1 has five rate constants. However, only four of the rate constants ($k_i$, $k_p$, $k_{vinylidene}$, and $k_{vinylene}$) were determined from optimization as the $k_{i,H}$ rate constant was fixed at $1000k_i$ on the basis of the assumption that Zr−H$^+$ species are quick to react as supported by Burger et al.,[45] who studied the reactivity of Sc−H$^+$ species, and Chirik and Bercaw,[46] who found Zr−H bonds to be extremely reactive toward most functional groups. The general bimolecular vinylene reaction, characterized by the single rate constant $k_{vinylene}$, was used in the PASM as it was considered sufficient for description of the vinlyene data in Figure 3. In addition to the four rate constants, the initial fraction of activated catalyst ($X_{active}$) defined as $X_{active}$ = [(EBI)ZrMe$^+$]$_0$/[(EBI)ZrMe$_2$]$_0$ was optimized.

Optimization of the full parameter set ($k_i$, $k_p$, $k_{vinylidene}$, $k_{vinylene}$, and $X_{active}$) was performed using the entire multiresponse data set presented in Figures 3−5 and the Supporting Information. The optimized values are reported in Table 1, with the predictions given by this parameter set already presented in Figures 3−5. It can be concluded that the PASM with a single set of parameter values is capable of describing all the multiresponse polymerization data, where it was found that 43% of the catalyst must remain inactive beginning in the initial stages of the polymerization and lasting for the duration of the reaction.

## Discussion

**PASM Validation.** The PASM, based on the mechanism given in Scheme 1 and a decreased amount of actively polymerizing

(45) Burger, B. J.; Thompson, M. E.; Cotter, W. D.; Bercaw, J. E. *J. Am. Chem. Soc.* **1990**, *112*, 1566–1577.

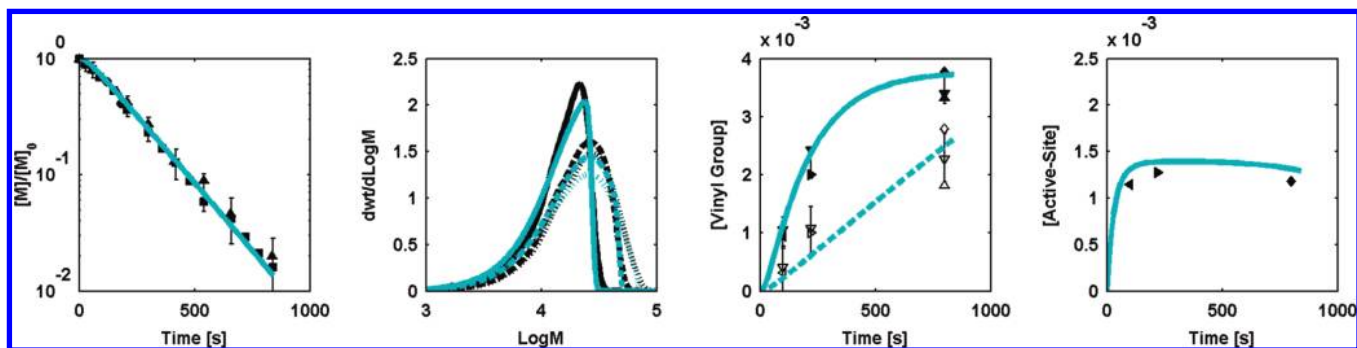(46) Chirik, P. J.; Bercaw, J. E. *Organometallics* **2005**, *24*, 5407–5423.

**Figure 3.** Monomer consumption, MWD (black solid line, 100 s; black dashed line, 220 s; black hatched line, 800 s), vinyl group concentration (vinylidene, open symbols; vinylene, solid symbols), and active site concentration data compared to the partial active site model (PASM) prediction (blue solid line, monomer and active site concentration; blue solid line, 100 s MWD; blue dashed line, 220 s MWD; blue hatched line, 800 s MWD; blue dashed line, vinylidene; blue solid line, vinlyene). Each symbol represents a unique polymerization experiment. Error bars represent 98% confidence intervals. Conditions: 0 °C, toluene, $[(EBI)ZrMe_2]_0 = [B(C_6F_5)_3]_0 = 2.49$ mM, $[\text{1-hexene}]_0 = 1.0$ M.
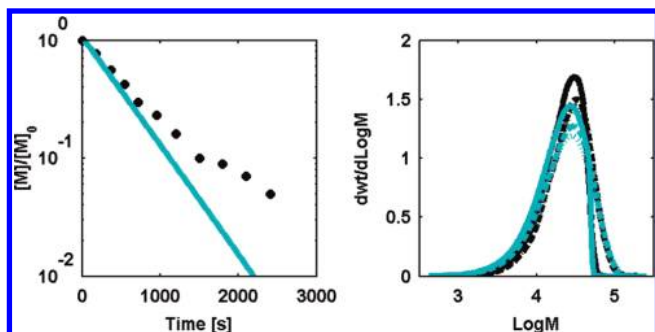


**Figure 4.** (Left) Monomer consumption (●) and (right) MWD at 180 s (23% monomer conversion) (black solid line), 540 s (58%) (black dashed line), and 1503 s (90%) (black hatched line) compared to the partial active site model (PASM) prediction prediction (blue solid line, monomer concentration; blue solid line, 180 s MWD; blue dashed line, 540 s MWD; blue hatched line, 1503 s MWD) (0 °C, toluene, $[(EBI)ZrMe_2]_0 = [B(C_6F_5)_3]_0 = 1.0$ mM, $[\text{1-hexene}]_0 = 1.0$ M).
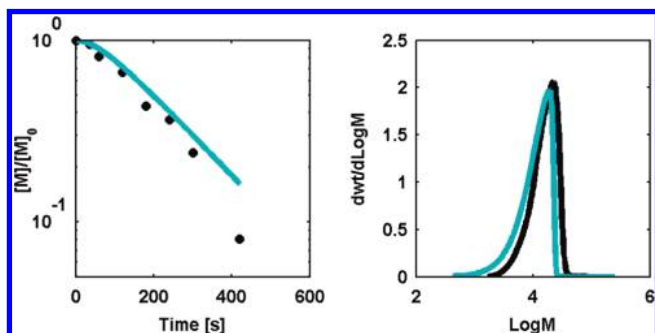


**Figure 5.** (Left) Monomer consumption (●) and (right) molecular weight distribution at 180 s (57% monomer conversion) (black line) compared to the partial active site model (PASM) prediction (blue line) (0 °C, toluene, $[(EBI)ZrMe_2]_0 = [B(C_6F_5)_3]_0 = 2.49$ mM, $[\text{1-hexene}]_0 = 0.5$ M).

catalyst, is able to describe the multiresponse polymerization data reported in this paper. In addition, the model can be used to predict the experimental MWDs originally reported by Landis et al.[20] and replotted in Figure 2. The prediction is given in Figure 6, with the corresponding monomer conversions reported in Table 3. It is clearly evident that the MWD prediction given by the PASM is significantly improved with no loss to the quality of the corresponding monomer conversion prediction.

The PASM successfully describes the entire multiresponse data set reported in the paper and also predicts the experimental MWDs and monomer conversion reported by Landis et al.;[20] however, a discrepancy must be acknowledged. Our experi-

mentally measured value of approximately 50% active sites is significantly less than the 85−95% reported by Landis and co-workers.[19] Our experimental active site data were obtained at higher conversions (30−90%), while the Landis et al.[19,20] data were measured at low conversions (<10%); however, this hardly seems like an appropriate explanation for the difference. Nevertheless, without restricting the amount of active catalyst from the initial stages of the polymerization to only 57%, neither the active site count (i.e., Figure 3) at higher conversions nor the MWDs (including those reported by Landis et al.[20]) are predicted. Two alternative models were hypothesized to reconcile this discrepancy (see the discussion later in this section), but in both cases they failed to provide the broad ability to predict the entire data set. Although currently there is no resolution of the Landis et al.[20] data for low conversion, the PASM is currently the most complete kinetic description of this catalyst system.

**Source of Fewer Active Sites.** Reactive impurities are a common explanation when less than the expected amount of a chemically active species is observed. However, the possibility that impurities are poisoning some of the catalyst in our system is unlikely on the basis of the following arguments. First, the purity of the catalyst as judged by ${}^1H$ NMR of the crystallized $(EBI)ZrMe_2$ species showed the catalyst to be quite pure with impurities of less than 5% (i.e., the detection threshold of the instrument), clearly less than the observed 43%. Second, the PASM robustly shows 43% of the catalyst is inactive despite changes in the initial monomer and activator concentrations. If an impurity is present in either of these, then halving/doubling the species amount should have given approximately 22%/65% inactive catalyst, respectively. Finally, the solvent as a source of impurities is eliminated as changes in either the reaction volume or initial concentration of catalyst consistently showed 43% of the catalyst inactive. Had an impurity in the solvent been the cause, the observed fraction of catalyst should have scaled with the changes in reaction volume or initial catalyst concentration.

With the possibility of reactive impurities eliminated, the source of the inactive catalyst now must be addressed. In the PASM it does not matter whether the catalyst is rendered inactive prior to activation, after activation prior to initiation, or simultaneous with initiation. Explanation of the catalyst inactivity as a result of incomplete activation is eliminated by activation studies which have conclusively shown that activation for this catalyst system is complete at activator to catalyst ratios
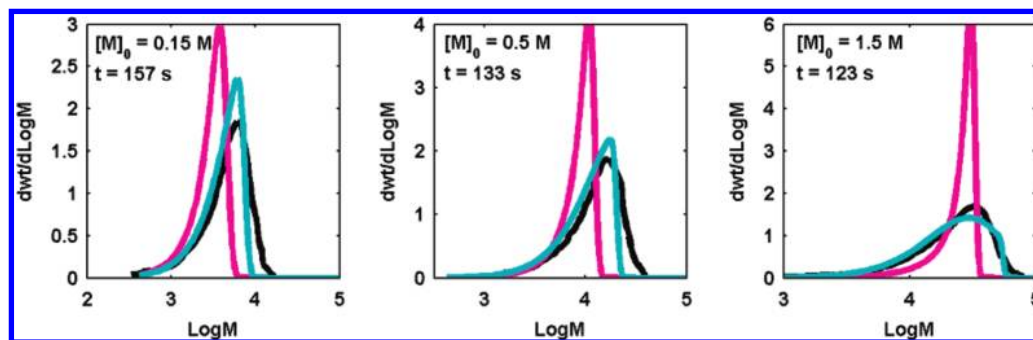
**Figure 6.** Digitized data from Landis et al.[20] (black line), Landis et al.[20] model prediction (blue line), and partial active site model (PASM) prediction (pink line) for three initial conditions (0 °C, toluene, $[(EBI)ZrMe_2]_0 = [B(C_6F_5)_3]_0 = 0.6$ mM).

**Table 3.** Monomer Conversion (%) for MWDs Reported in Figure 6[a]

| $[M]_0$ (M) | sample time (s) | exptl[b] | Landis et al.[20] prediction | PASM prediction[c] |
|---|---|---|---|---|
| 0.15 | 157 | 7 | 6 | 6 |
| 0.5 | 133 | 11 | 10 | 9 |
| 1.5 | 123 | 10 | 13 | 12 |

[a] Conditions: 0°C, toluene, $[(EBI)ZrMe_2]_0 = [B(C_6F_5)_3]_0 = 0.6$ mM). [b] Obtained from Landis et al.[20] [c] PASM = partial active site model.

of 1:1 and greater.[20,47] This observation was verified by our group, and the $^1H$ NMR data can be found in the Supporting Information. The remaining two options both lead to the conclusion that the source of only a partial number of catalyst sites being active is a catalytically significant event that impacts the subsequent polymerization as evidenced by the MWD. Work is ongoing in our group to elucidate the mechanistic details of this catalytic event.

**Robustness of Rate Constant Values.** Confidence intervals have yet to be assigned to the optimized rate constants given in Table 1. Linear statistical analysis is not appropriate because of the inherent nonlinearity of the problem. Nonlinear Bayesian statistical analysis can provide an insightful look at the confidence regions and correlations between rate constants, but that more sophisticated analysis is beyond the scope of this paper. In the absence of such a nonlinear statistical analysis, the robustness of the rate constants has been assessed considering the impact of systematic errors in the MWD and alteration of the data weighting scheme used in optimization.

One method used to probe the robustness of the parameter values was to consider the impact of systematic errors in the MWD. The effect of four potential systematic errors on the position and shape of the MWD were considered: (i) a 10% increase and (ii) a 10% decrease in d$n$/d$c$ associated with an error in sample concentration, (iii) alteration of the integration range/baseline by resolving the baseline post solvent peak (compared to pre-solvent peak), and (iv) decreasing the inter-detector delay time by 1 s (see the Supporting Information for details). For each systematic error, the error was incorporated into the experimental MWDs and the optimization was rerun. The modified values of the rate constants and $X_{active}$ were then compared to the original optimized results. The various systematic errors give similar fit qualities of the data as reflected in the comparable sum of squared errors. In all cases the rate constants and $X_{active}$ varied by ≤12%. This result indicates that the parameter values extracted from this data set are only minimally sensitive to the systematic errors in the MWDs that

may occur during GPC analysis. We note that this conclusion may not universally extend to other catalyst systems governed by a different mechanism, where sensitivity to experimental errors in the MWD determined via GPC may be more significant.

Another evaluation of the robustness of the rate constants was performed by examining the sensitivity to the weight of the various types of data in specifying the objective function used in the parameter optimization. This highlights how the uncertainty in the different types of data is reflected in the value of the rate constants. If the data are without error, a change in weighting will have no impact on the value of the rate constants. As shown in the Supporting Information, changes in the weighting scheme resulted in minimal changes to the quality of the fit and the parameter values show a minimal sensitivity. With the exception of a 16% change in $k_i$ when each type of data was given an equal weight, changes of 6% or less were observed in the different weighting schemes. Details are provided in the Supporting Information.

As shown in Table 1, the rate constants reported in this paper are significantly different as compared to those previously deduced from independent analysis of multiresponse data by Landis et al.[20] A $k_p$ of 3.7 $M^{-1}$ $s^{-1}$ was determined from the multiresponse data, which is 1.7 times greater than the $k_p$ of 2.2 $M^{-1}$ $s^{-1}$ originally reported by Landis et al.[20] While this increase is not large, the robustness of the rate constants obtained herein highlights the ability of comprehensive, quantitative modeling applied to rich multiresponse data to do much better than just order-of-magnitude estimates of the rate constants. The analysis described above clearly indicates that the difference in $k_p$ between 2.2 and 3.7 $M^{-1}$ $s^{-1}$ is real and significant. This is highlighted by the inability of the original $k_p$ to predict the MWD, while a $k_p$ 1.7 times greater (in conjunction with other modified rate constants) does predict the MWD. This refined set of rate constants determined by comprehensive, quantitative kinetic modeling of a rich multiresponse data set is essential for building predictive structure−activity relationships where differences by a factor of 2 have already shown significance in structure−activity relationships as given by Manz and co-workers.[15]

The $k_i$ found in the PASM is consistent with that previously reported by Landis et al.[20] The chain transfer rate constants are significantly higher than those previously reported.[20] A factor of 2 difference in $k_{vinylidene}$ and $k_{vinylene}$ can be attributed to the number of active sites being decreased by approximately half. The remaining difference in the two chain transfer rate constants is a result of the significantly greater amount of double bonds observed in our data at higher monomer conversions than was

(47) Stahl, N. G.; Salata, M. R.; Marks, T. J. *J. Am. Chem. Soc.* **2005**, *127*, 10898–10909.

measured previously during the initial stages of the polymerization (i.e., less than 10% monomer conversion).[20]

**Alternative Model Possibilities.** The PASM is the simplest model we have been able to construct that is capable of describing the entire data set. It is important to remember that it is never possible to prove a model; rather, the scientific method can only disprove a specific hypothesis, where a not yet considered hypothesis could also describe the data.[48,49] Thus, what kinetic models of comparable or greater simplicity can describe the data? Instead of assuming 43% of the catalyst is inactive, is there an alternative explanation? While an exhaustive list of all the models we have examined and have shown to be unsatisfactory is not appropriate in this paper, a discussion of several of the discarded models is warranted.

One alternative hypothesis to describe the data is to assume that 100% of the catalyst activates but a deactivation occurs during the course of the reaction. The idea behind this is to allow the 85−95% activation seen by Landis at the beginning of the reaction and then allow catalyst deactivation to decrease the amount of catalyst to agree with our measured 57% active site count at higher conversions. This model can be quickly discarded on the basis of the linearity of the semilog monomer consumption data and the MeOD quench data giving the same concentration of active catalyst at 30%, 60%, and 90% monomer conversion. Both these results contradict time-dependent deactivation as catalyst deactivation would have to cease at 30% and the remaining catalyst would need to increase its propagation rate to maintain the constant rate of polymerization.

A second possible hypothesis is a punctuated chain transfer mechanism, where punctuation refers to the idea that the catalyst species remaining after chain cleavage is slow to reinitiate growth of a new chain compared to the rate of propagation. This is in direct contrast to the assumption that the zirconium hydride species ($Zr-H^+$) produced by $\beta$-hydride elimination is fast to reinitiate. The mechanism of punctuated chain transfer could refer to either a case in which the $Zr-H^+$ is slow to reinitiate or an alternative, yet not understood, chain transfer pathway. Both punctuated chain transfer mechanisms seem very attractive as they appear to allow for 85−95% of sites activating, but then predict fewer active sites as the amount of punctuated catalyst accumulates. The argument against this model is subtle. Landis et al.[19] performed two different types of active site count probing: (i) the total number of sites that have been or are currently active and (ii) only the number of sites currently active. They found the two experiments yield identical results, implying the number of currently active sites is equal to the total number of sites ever activated.[19] In contrast, the punctuated chain transfer reaction predicts that the results of these two experiments should be different, with the number of currently active sites never exceeding 57%.

To summarize, we have examined a number of polymerization mechanisms other than the PASM and have found them unable to describe the data. Specifically, among the mechanisms examined were time-dependent catalyst deactivation and punctuated chain transfer, which offered the most promising alternative hypotheses to describe the multiresponse data set. However, as discussed above, both were found inadequate in describing all the data. The proposed PASM is the simplest model that is chemically reasonable and is able to quantitatively describe the full set of multiresponse data for 1-hexene polymerization catalyzed by (EBI)ZrMe$_2$ activated with B(C$_6$F$_5$)$_3$.

## Conclusions

While individual experiments to probe specific mechanisms have heretofore been insightful in understanding single-site catalysts, a higher fidelity mechanistic picture can be determined by the comprehensive, quantitative kinetic modeling of multiresponse data. For 1-hexene polymerization by (EBI)ZrMe$_2$/B(C$_6$F$_5$)$_3$, individual experiments were successful at elucidating a number of features in the mechanism, e.g., chain transfer mechanisms,[20] continuous versus intermittent propagation,[41] and the reactivity of 2,1-misinserted species.[39] However, inclusion of the MWD in the multiresponse data revealed 43% of the catalyst is inactive from the initial stages of polymerization. Furthermore, it could be deduced that the catalyst inactivity was not a result of impurities or incomplete activation, but rather a catalytically significant event. In addition, the simultaneous kinetic modeling produced robust values of the rate constants with uncertainties of less than 16%. Finally, it is quite possible that this phenomenon occurs in other single-site polymerization catalyst systems, but has been hitherto overlooked as a result of insufficient kinetic modeling of these systems. The addition of comprehensive, quantitative kinetic modeling to the arsenal of spectroscopic tools that are currently used to study single-site polymerization kinetics provides the opportunity for significant enhancement in the determination and discrimination of fundamental kinetic mechanisms.

**Supporting Information Available:** GPC analysis details and error assessment, error analysis for additional types of data, data weighting scheme, kinetic model equations, additional data with model predictions, and $^1$H NMR of catalyst activation. This material is available free of charge via the Internet at http://pubs.acs.org.

JA906332R

(48) Popper, K. R. *The Logic of Scientific Discovery*; Basic Books, Inc.: New York, 1959.
(49) Platt, J. R. *Science (Washington, DC, U.S.)* **1964**, *146*, 347–353.